

Formation and Study of Electrosark Coatings Based on Titanium Aluminides

S. A. Pyachin^a, A. A. Burkov^a, and V. S. Komarova^b

^a*Institute for Materials Science, Khabarovsk Scientific Center, Far East Branch, Russian Academy of Sciences,
ul. Tikhookeanskaya 153, Khabarovsk, 680042 Russia*

^b*Kosygin Institute of Tectonics and Geophysics, Far East Branch, Russian Academy of Sciences,
ul. Kim Yu Chen 65, Khabarovsk, 680000 Russia*

Received September 27, 2012

Abstract—Coatings containing Ti–Al intermetallics are fabricated by the electrosark deposition of titanium on aluminum and aluminum on titanium. The microstructure and composition of the grown coatings is studied by scanning electron microscopy, X-ray diffraction, and S-ray microanalysis. It is found that the surface layer formed in argon mostly contains the α -TiAl₃ intermetallic independent of the duration and frequency of discharge pulses. The γ -TiAl and α_2 -Ti₃Al phases can be obtained by aluminum deposition on titanium followed by the subsequent deposition of a second titanium layer. Aluminum oxide and titanium nitride are additionally formed during the deposition of electrosark coatings in air.

DOI: 10.1134/S1027451013030336

INTRODUCTION

Alloys based on Ti–Al intermetallics are of particular interest as promising structural materials for the aerospace and automobile industries due to their unique properties, e.g., high melting temperature, low density, high elastic modulus, heat, oxidation, and ignition resistance [1, 2]. Furthermore, there is the tendency to use titanium aluminides to develop protective and wear-resistant coatings. A TiAl layer deposited onto a pseudo- α -titanium alloy makes it high-temperature oxidation resistant while retaining its protective properties when stretching the titanium substrate [3]. The Ti₃Al-containing coating on a titanium surface has excellent wear resistance due to its increased hardness. A similar coating based on a TiAl₃ + TiAl mixture exhibits high oxidation resistance [4]. Thus, phase modifications of Ti–Al compounds make it possible to control the properties of intermetallic coatings, which is achieved in practice by choosing the methods and conditions of their deposition.

Currently, there is a large number of methods for growing intermetallic coatings. Among them are magnetron sputtering [3, 5], vacuum-arc deposition [6, 7], ion implantation [8–11], gas–plasma deposition [12, 13], laser cladding [4, 14, 15], electron-beam coating [16], and others. Most of these methods are based on material condensation from the vapor phase in vacuum or Ti–Al substrate surface bombardment by particles, or molten-state mixing of the substrate surface layer with a preliminarily deposited material. As a rule, additional annealing is required to homogenize the structure of the obtained coatings. In this study, we fabricated coatings based on titanium aluminides

using the electrosark alloying method based on metal transfer from anode to cathode during multiply repeated electric discharges. This technology has some advantages over other methods [17–19]. First of all, these are the technological simplicity of metal deposition in a gas medium at atmospheric pressure, the homogeneous composition of the surface layer due to molten-state mixing of the materials used as electrodes, and high coating–substrate adhesion. The composition of the grown coatings is controlled in many respects by the technological parameters of deposition; however, since they are almost unknown for electrosark Ti–Al intermetallic coatings, additional studies are required. The objective of this study is to determine the main features of the formation of electrosark coatings based on titanium aluminides with tailored stoichiometric ratios. To solve the posed problem, the effect of the total deposition time, frequency, discharge-pulse length, and gas atmosphere on the phase composition of the intermetallic coatings is studied.

EXPERIMENTAL

The electrosark-coating deposition process is schematically shown in Fig. 1. Discharge pulses were supplied by a generator based on a circuit of controlled transistor gates [20] and were fed to a vibrator with an alloying electrode (anode). The vibration device was used to initialize electric discharges at the instant of anode–cathode (substrate) contact breaking, since the applied voltage (below 50 V) was insufficient for inter-electrode gas-gap breakdown. The anode oscillation frequency was chosen from the range of 100–300 Hz so

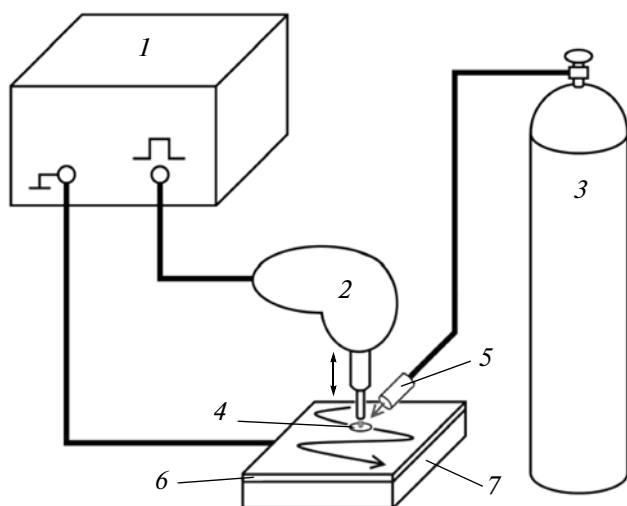


Fig. 1. Schematic representation of electrospray-coating deposition: (1) discharge-pulse generator, (2) manual vibrator with anode, (3) gas cylinder, (4) discharge exposed area, (5) nozzle, (6) coating, and (7) substrate (cathode).

as to exclude electrode seizure upon cooling of the molten metal. Since the electric discharge locally affects an area ~ 1 mm in diameter, the anode was moved back and forth along a meander-like curve along the cathode surface, which provided its uniform processing. The coatings were deposited in air at atmospheric pressure or in a protective gas atmosphere (argon). In the latter case, the area exposed to the discharge was cooled via a nozzle with argon fed from a gas cylinder.

During the experiments, the pulse repetition rate f was from 0.1 to 1 kHz. The discharge time τ was 80–400 μ s. The current pulse amplitude was 110 ± 10 A; the interelectrode voltage was 30 ± 5 V. The average power released during the discharge was 3.3 ± 0.8 kW. The coatings were deposited in argon or in air. Pure titanium and aluminum cylindrical rods 3.5 mm in diameter were used as anodes. Aluminum (AK8 alloy) plates $1 \times 1 \times 0.5$ cm in size and titanium (VT20 alloy) cylinders 11 mm in diameter and 5 mm in height were used as cathodes. The coatings were grown by the electrospray deposition of aluminum onto titanium and titanium onto an aluminum substrate. In some cases, Ti and Al were alternately deposited on the same sample.

Metallographic studies of the deposited layers were performed using a MIM-10 optical microscope. Furthermore, the coating microstructure was studied using an EVO 40HV scanning electron microscope in the phase contrast mode. Microprobe elemental analysis was performed using an INCA ENERGY 350 energy-dispersive spectrometer incorporated into the electron microscope. The phase composition of the metal surface layers was studied using a DRON-7 X-ray diffractometer in $\text{CuK}\alpha$ radiation. X-ray spectral lines were identified using the PDWin software pack-

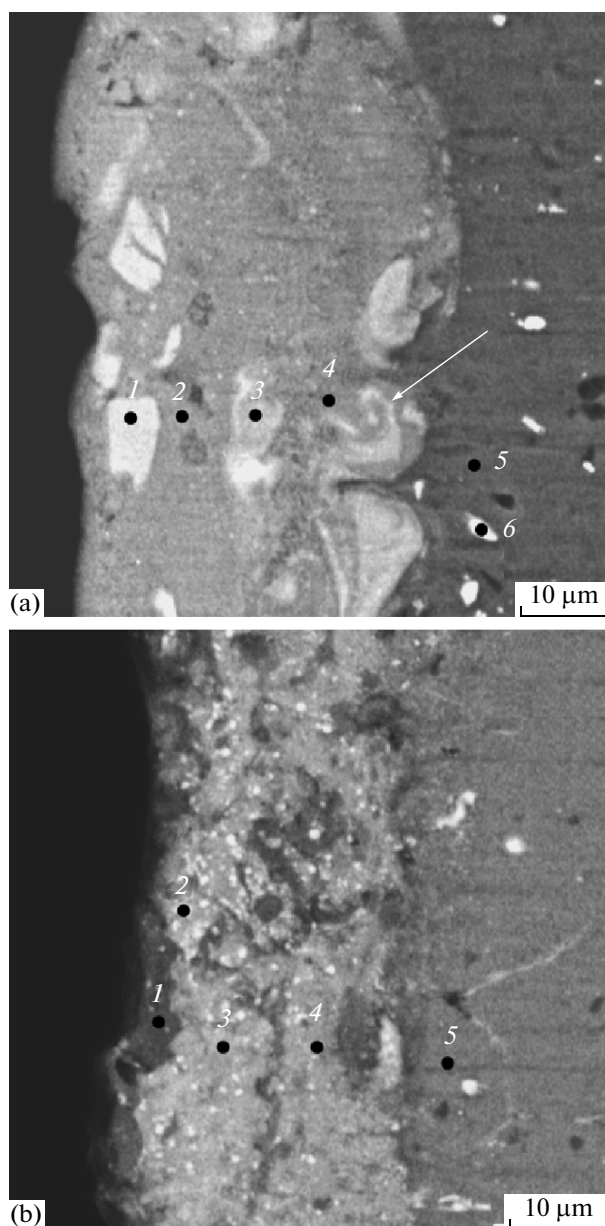


Fig. 2. Microstructures of the titanium coatings deposited onto an aluminum substrate in (a) argon and (b) air.

age (Burevestnik Company). The coating thickness was measured using a CALLTEST abrasive wear device.

RESULTS

Titanium Deposition onto Aluminum

The study of electrospray-produced titanium coatings on an aluminum substrate showed that the gas atmosphere during deposition has an effect on the microstructure and phase composition of the formed layers. Figure 2 shows scanning electron microscopy images of the cross sections of the coatings grown in

Table 1. Concentrations of elements (at %) at various points of the titanium coatings on aluminum

Point number	Elements								
	Al	Ti	Mn	Cu	Mg	Fe	Si	N	O
Fig. 2a	Argon								
1	59.0	39.1	0.6	1.3	—	—	—	—	—
2	74.5	21.4	0.5	2.3	1.3	—	—	—	—
3	69.8	27.7	0.7	1.8	—	—	—	—	—
4	84.4	10.8	0.4	2.6	1.8	—	—	—	—
5	96.4	—	0.4	2.1	1.1	—	—	—	—
6	72.6	—	3.5	7.3	—	11.4	5.2	—	—
Fig. 2b	Air								
1	44.8	16.9	0.4	1.5	—	0.4	—	16.5	19.6
2	34.3	2.6	—	—	1.9	0.4	—	12.1	48.6
3	66.8	16.8	—	1.4	1.1	0.4	—	—	13.5
4	58.4	19.5	0.3	1.8	—	0.7	—	—	19.3
5	92.3	3.1	0.3	1.9	1.3	—	—	—	1.1

argon and air. We can see that the surface layer differs in the structure from the substrate and consists of a mixture of phases of different densities. The chemical composition of various areas indicated by numbered points in Fig. 2 is presented in Table 1. Comparing the concentrations of detected elements, it was found that the average ratio of Ti and Al atomic concentrations in most areas of the surface layers (light gray areas, Fig. 2a, point 2 and Fig. 2b, points 3 and 4) is $\sim 1 : 3.48$ which is close to the ratio of elements in the α -TiAl₃ intermetallic. In the coatings grown in argon, areas with a higher titanium content are observed (bright areas in Fig. 2a, point 1), in which the atomic concentration ratio Al : Ti is in the range of 1.5–2.5, i.e., close to the stoichiometry of the TiAl₂ intermetallic. With distance from the sample surfaces to the substrate, the titanium content insignificantly decreases, while the aluminum concentration increases. Noteworthy is that frozen convective material flows can be distinguished in the deposited surface layer, which promote metal mixing and homogenization of the coating composition. White spots in the aluminum-alloy substrate area correspond to inclusions with increased iron and silicon contents (Fig. 2a, point 6).

The formation of TiAl₃ as the basic intermetallic in electrospark-produced titanium coatings on aluminum independent of deposition conditions was confirmed by X-ray diffraction studies. Figure 3 shows the X-ray spectra of the obtained coatings. The peak intensities are given in relative units. The X-ray spectra of the coatings deposited in argon contained α -TiAl₃ and aluminum lines. The absence of titanium lines in

the X-ray diffraction patterns of the coatings is explained by the fact that all of the titanium transferred from the anode interacts with aluminum.

The deposition of a titanium coating in air is accompanied by its oxidation, which is caused by the

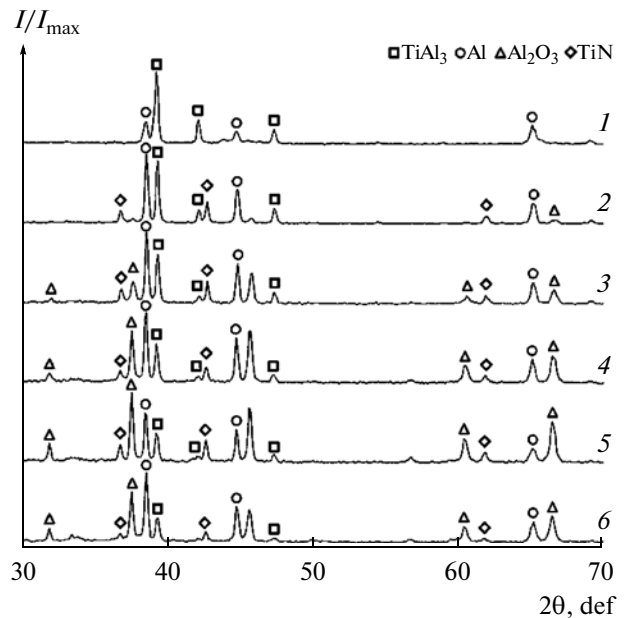


Fig. 3. X-ray diffraction patterns of the titanium coatings deposited onto aluminum in various media in (1) 4 min, argon; (2) 2 min, air; (3) 6 min, air; (4) 10 min, air; (5) 16 min, air; (6) 20 min, air; $\tau = 200 \mu\text{s}$, $f = 500 \text{ Hz}$.

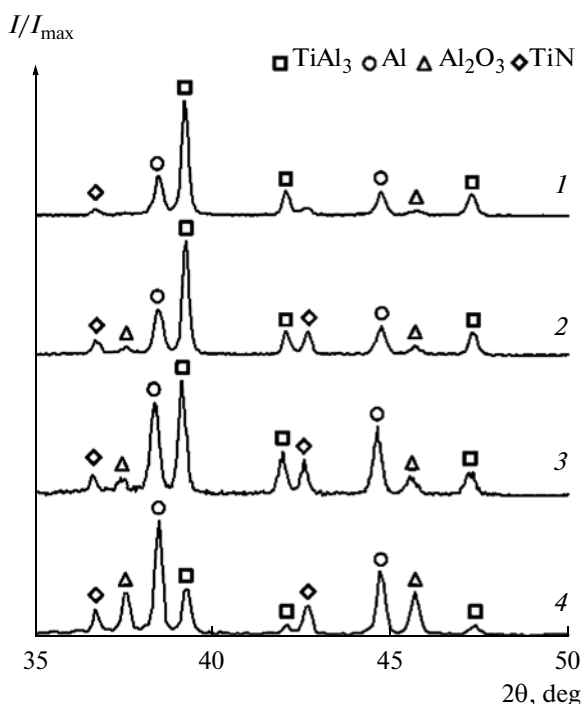
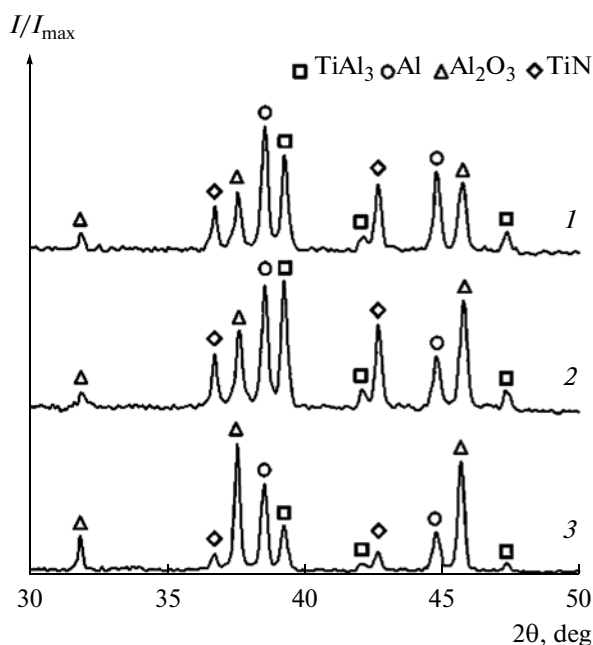
Table 2. Thickness of the titanium coating on the aluminum substrate as a function of the electrospark-deposition time in air ($\tau = 200 \mu\text{s}$; $f = 500 \text{ Hz}$)

Time, min	0	2	4	8	10	12	16	20
Average thickness, μm	0	28	32	44	46	80	110	60

interaction of electrode materials with the components of air. Additional Al_2O_3 and TiN peaks appear in the X-ray diffraction patterns of such coatings. We note that titanium-dioxide reflections were not observed in the spectra, which is explained by the more favorable thermodynamic conditions for titanium-nitride formation at the temperatures reached in the area exposed to the discharge, in comparison with its oxides. According to estimates, the Gibbs free energy of TiN (-239 J/mol) is lower than that of TiO (-201 J/mol) at a temperature of 2000 K. X-ray microanalysis showed that an increased aluminum-oxide concentration is observed in the surface layer regions colored by dark gray in Fig. 2b (point 1). As a rule, these regions have elongated shapes. Bright round spots (point 2) correspond to higher titanium-nitride concentrations. TiN clustering regions $\sim 1 \mu\text{m}$ in diameter are uniformly distributed over the entire coating. As the deposition time increases, the reflection intensities in the TiN and Al_2O_3 X-ray diffraction patterns increase to 16 min and then decrease. This is

caused by the intense destruction of the surface layer due to defect accumulation. Table 2 shows that the coating thickness increases in the first deposition stages and then decreases. This effect is known as the onset of the “brittle-fracture threshold” [17]; therefore, the electrospark coatings are deposited before this instant.

The effect of the discharge-pulse length on the phase composition of the coatings deposited in air is as follows: as τ increases from 80 to 400 μs , the Al_2O_3 and TiN content becomes larger in comparison with $\alpha\text{-TiAl}_3$ (Fig. 4). This means that the time the “metal-air” system is in the high-temperature region increases with the duration of multiply repeated discharges, which increases the reaction rates of the interaction of titanium and aluminum with nitrogen and oxygen. X-ray diffraction patterns of the coatings grown in air at various repetition rates of discharge pulses for a constant numbers of discharges and durations of 2.4×10^5 and 100 μs , respectively, are shown in Fig. 5. We can see that, as the discharge frequency increases from

**Fig. 4.** X-ray diffraction patterns of titanium coatings on aluminum, deposited in air at discharge times of (1) 80, (2) 160, (3) 280, and (4) 400 μs ; $f = 250 \text{ Hz}$, $t = 4 \text{ min}$.**Fig. 5.** X-ray patterns of the titanium coatings deposited onto an aluminum substrate in air at frequencies of (1) 100, (2) 200, and (3) 500 Hz. $\tau = 100 \mu\text{s}$. The number of discharges is $N = 2.4 \times 10^5$ pulses.

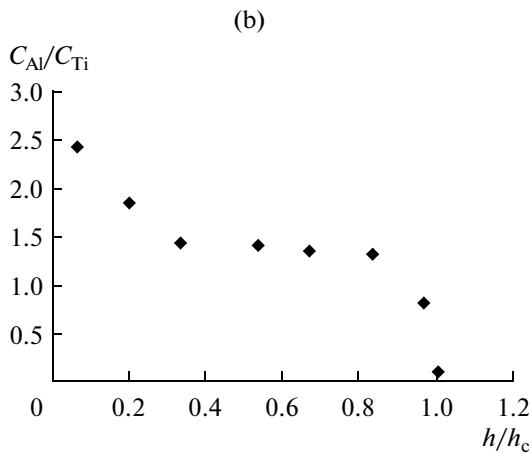
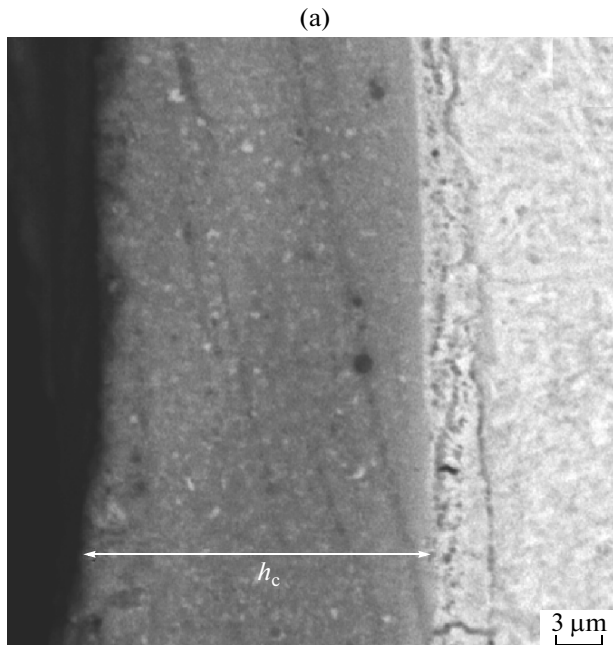


Fig. 6. (a) Microstructure of the cross metallographic section of the aluminum coating on titanium and (b) the ratio of aluminum and titanium atomic concentrations as a function of the depth reduced to the coating thickness h_c .

100 to 500 Hz, the aluminum-oxide content becomes higher relative to titanium nitride and α -TiAl₃. This fact can be explained by more intense heating of the aluminum substrate at increased frequencies. Titanium aluminides of other stoichiometric compositions than TiAl₃ were not detected. Thus, the electric-discharge duration and frequency affected, first of all, the quantitative content of compounds in the coating, rather than its qualitative composition.

Aluminum Deposition onto Titanium

The microstructure of the aluminum coating on titanium, deposited in argon, is shown in Fig. 6a. The deposited layer is more homogeneous, and it contains a smaller number of cracks and pores in comparison

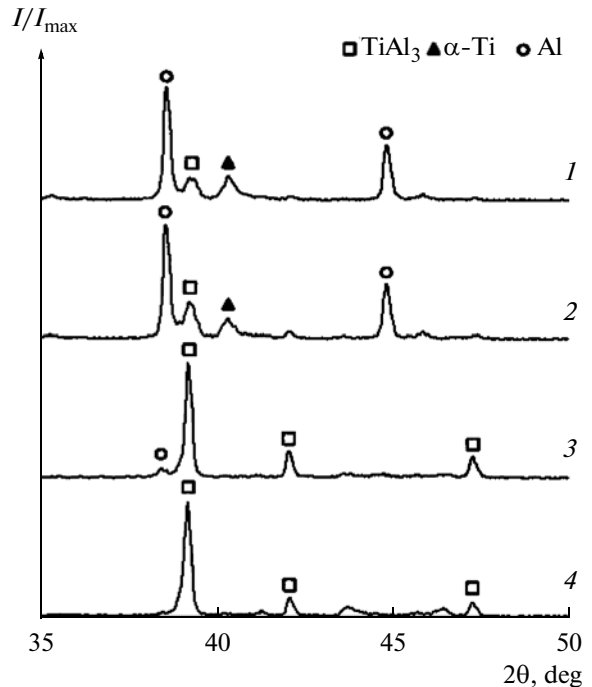


Fig. 7. X-ray diffraction patterns of the aluminum coatings deposited onto titanium in argon in (1) 1, (2) 2, (3) 3, and (4) 4 min; $f = 1000$ Hz, $\tau = 300$ μ s.

with the titanium coating on aluminum. Furthermore, inclusions (open circles in the coating) smaller than 1 μ m in diameter and of higher density than the basic coating material are observed. According to the X-ray microanalysis data, the ratio of atomic concentrations in these regions is close to unity, i.e., they are γ -TiAl intermetallic cluster regions. The layer thickness for 4-min deposition reaches 20–40 μ m. The titanium and aluminum concentrations differ at various depths. Figure 6b shows the variation in the average ratio of the Ti and Al atomic concentrations as a function of the distance from the sample surface, reduced to the coating thickness. We can see that the ratio of the concentrations of these elements in the upper layers of the coating is close to that of the TiAl₃ intermetallic; in deeper layers, it is close to that of the TiAl intermetallic. However, this probably results from an increased titanium content, rather than an increase in the TiAl content.

X-ray diffraction analysis of the upper layers of the aluminum coatings on titanium, grown at short (less than 2 min) deposition times in argon, showed that they consist of a set of phases, Al, Ti, and TiAl₃ (Fig. 7). As the total deposition time and the number of pulses increase, the time that the material is in the molten state increases; therefore, the deposited metal is actively mixed with substrate material. This results in an increased content of the α -TiAl₃ phase. However, due to coating thickening, bulk titanium emergence in the surface layers becomes more compli-

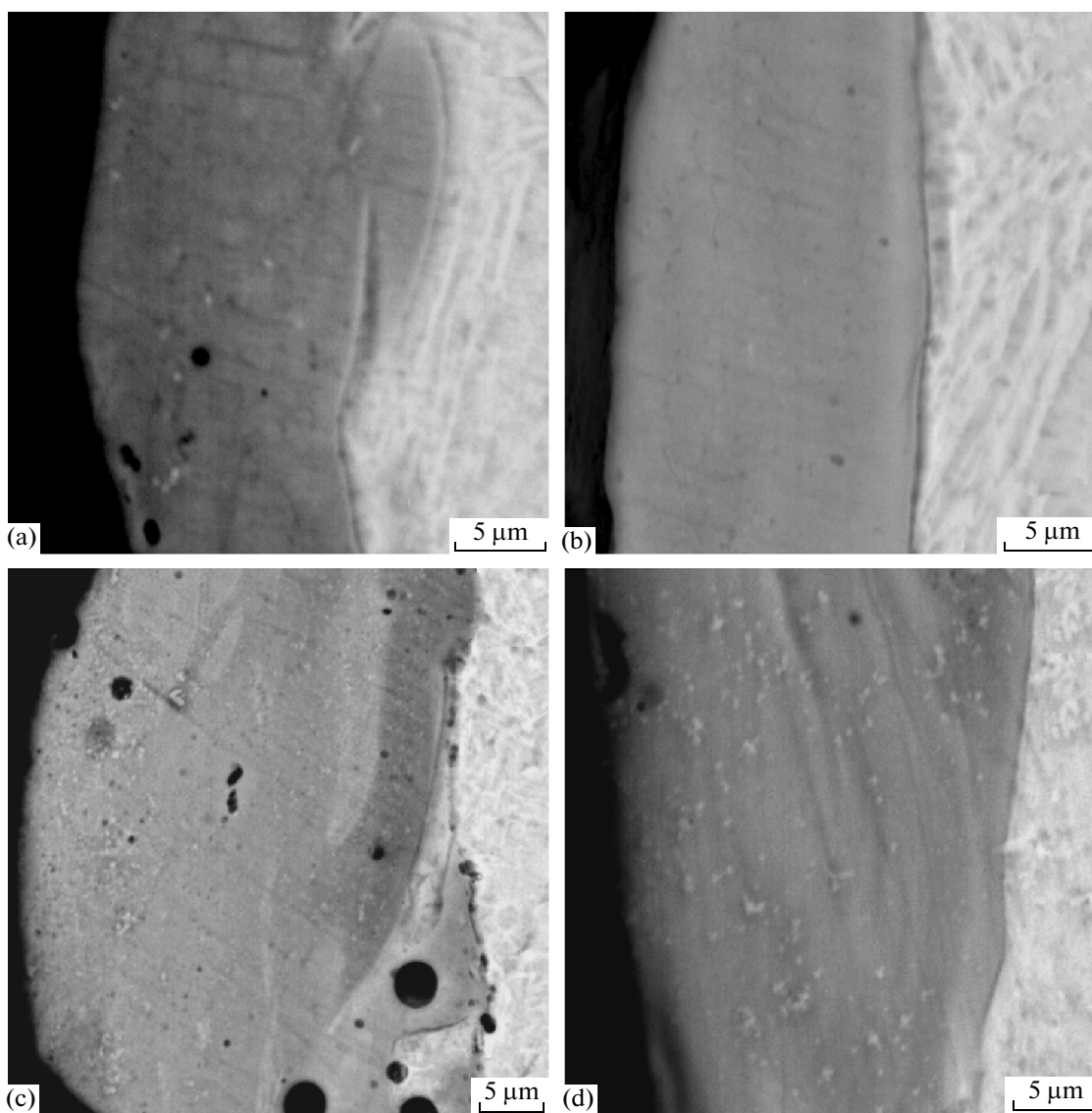


Fig. 8. Scanning electron microscopy images of cross sections of the electrospark-produced aluminum coatings on titanium with additional titanium deposition. Metal deposition times in argon are (a) 2 min Al and 1 min Ti, (b) 3 min Al and 1 min Ti, (c) 4 min Al and 1 min Ti, (d) 3 min Al and 3 min Ti; $f = 1000$ Hz, $\tau = 300$ μ s.

cated; therefore, intermetallics of other stoichiometric ratios are not formed. Similar coatings grown in air, in addition to the above-listed phases, contained aluminum oxide whose content increased with the deposition time. As in the previous case, changes in the discharge duration and frequency had no significant effect on the qualitative composition of the coatings.

Aluminum Deposition onto Titanium with Additional Titanium Deposition

The above experiments showed that the titanium content is insufficient to obtain the Ti_3Al compound; therefore, we proposed the growth of combined coatings by the sequential deposition of aluminum and titanium. The first aluminum layer was deposited onto

titanium in various times from 1 to 4 min; the second titanium layer was deposited in 1–3 min. The microstructure of the coatings grown in argon during sequential aluminum deposition onto titanium for various deposition times is shown in Fig. 8. Despite the two-stage deposition of the metals, combined coatings did not exhibit a pronounced layered structure, which is explained by strong mixing of the material in the molten state. In general, the coating thickness increases with the aluminum deposition time and reaches ~ 50 μ m in 4 min. The deposited layer contains small (< 1 μ m in diameter) inclusions of increased density, in which the titanium concentration is slightly higher than the aluminum concentration.

X-ray diffraction spectra of the combined coatings are shown in Fig. 9. The coating composition is char-

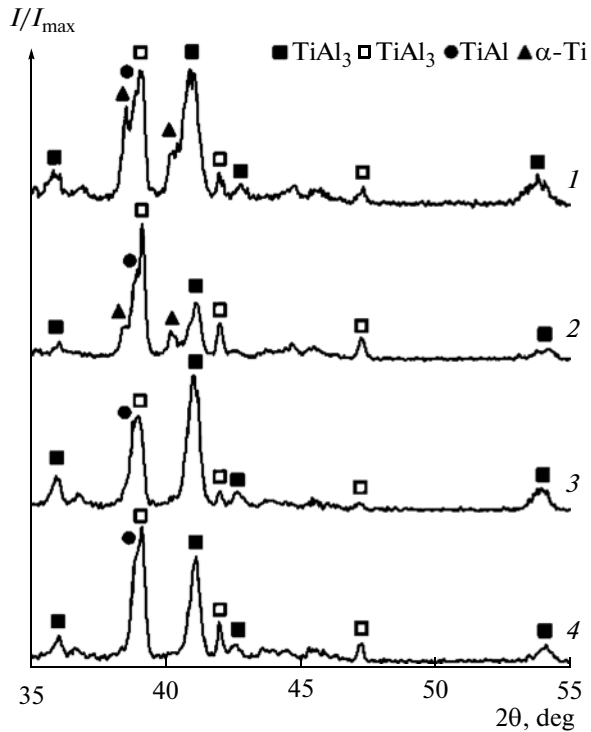


Fig. 9. X-ray diffraction patterns of the combined aluminum and titanium coatings on the titanium substrate. The deposition time of the first aluminum layer: (1) 1, (2) 2, (3) 3, and (4) 4 min. The deposition time of the second titanium layer is 1 min. Argon atmosphere; $f = 1000$ Hz, $\tau = 300$ μ s.

acterized by the presence of three main phases: Ti, TiAl_3 , Ti_3Al , and TiAl. As the deposition time of the first aluminum layer increases from 1 to 4 min, the titanium content decreases, and the TiAl and TiAl_3 intermetallic content remains approximately at the same level. As the deposition time of the second titanium layer increases, Ti_3Al becomes a major phase. However, during 3-min Ti deposition, the α -titanium content appreciably increases, while intermetallic concentrations decrease (Fig. 10); therefore, it is inexpedient to deposit the second titanium layer in longer than 2 min.

X-ray microanalysis showed that the chemical compositions of the combined coating regions at various distances from the sample surface differ depending on the deposition time of the aluminum and titanium layers (Fig. 11). If the first aluminum layer was deposited in 2 min and the following titanium layer was deposited in 1 min, the average ratio of Al and Ti atomic concentrations in the coating was close to 0.5, i.e., the titanium content was larger in comparison with aluminum. As the deposition time of the first Al layer was increased to 4 min, the Al content in the coating increased; the Al : Ti concentration ratio shifted toward aluminum and reached 2.3, which indicated the dominance of γ TiAl and α_2 - Ti_3Al . In the

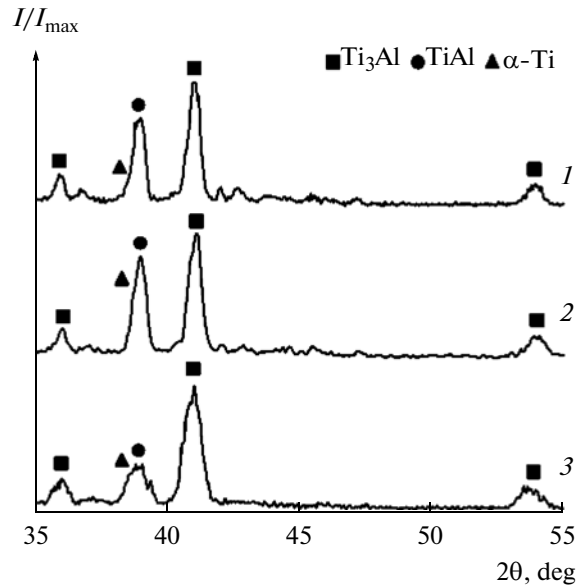


Fig. 10. X-ray diffraction patterns of the combined aluminum and titanium coatings on the titanium substrate. The deposition time of the first aluminum layer is 3 min. The deposition time of the second titanium layer is (1) 1, (2) 2, (3) 3, and (4) 4 min. Argon atmosphere; $f = 1000$ Hz, $\tau = 300$ μ s.

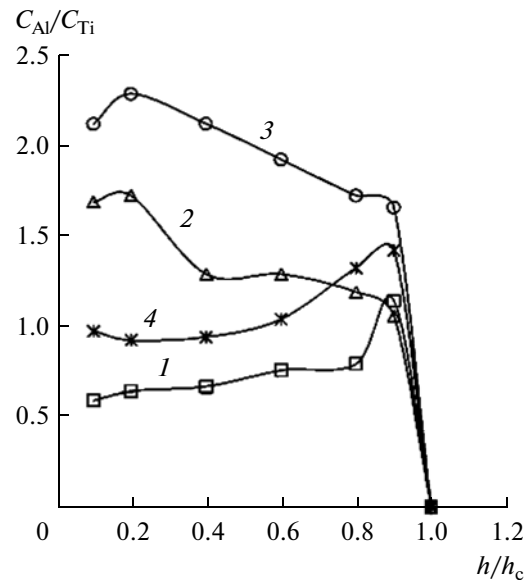


Fig. 11. Average ratios of atomic concentrations of aluminum and titanium as functions of the depth reduced to the combined coating thickness h_c . The time of metal deposition in argon is (1) 2 min Al and 1 min Ti, (2) 3 min Al and 1 min Ti, (3) 4 min Al and 1 min Ti, (4) 3 min Al and 3 min Ti. $f = 1000$ Hz, $\tau = 300$ μ s.

surface layers of the coating, the relative aluminum concentration insignificantly decreased due to the incompletely mixed second titanium layer. An increase in the deposition time of the second titanium

layer caused a consequent decrease in the ratio of the Al and Ti atomic concentrations. In the case of 3-min aluminum deposition and 3-min titanium deposition, the ratio was close to unity. It should also be noted that the aluminum concentration was higher near the “coating–substrate” boundary at approximately equal titanium and aluminum deposition times (lines 1 and 4 in Fig. 11). This is probably caused by the fact that the time the titanium is in the molten state is insufficient to completely overcome the preliminarily deposited aluminum layer.

CONCLUSIONS

The formation of titanium aluminides in coatings deposited by the electrospark alloying method was studied. It was shown that α -TiAl₃ is as a rule formed during titanium deposition onto aluminum and aluminum deposition onto titanium in argon. In the case of alloying in air, titanium nitride and aluminum oxide are additionally formed. The thickness of the electrospark coatings is limited due to the formation of brittle phases, defect accumulation, and surface-layer destruction under cyclic thermomechanical loads. The discharge duration and frequency affect only the quantitative ratios of phases. The intermetallics γ TiAl and α_2 -Ti₃Al can be obtained by depositing a second titanium layer over the aluminum coating on the titanium substrate. Composite coatings with a dominant concentration of one of the intermetallics of the “titanium–aluminum” system can be grown by varying the electrospark deposition time of the first aluminum layer and the second titanium layer. The properties of the obtained intermetallic coatings are planned to be studied in further works.

ACKNOWLEDGMENTS

The authors are grateful to L.P. Metlitskaya (Institute for Materials Science, Khabarovsk Scientific Center) and A.V. Bolokhovtsev (Pacific State University) for assistance in the fabrication and study of the samples.

This study was supported by the Presidium of the Far East Branch of the Russian Academy of Sciences (project no. 12-I-P8-02 “Physicochemical Features of the Formation of Ultrafine and Nanostructured Composite Materials and Coatings Based on Titanium Aluminides and Study of their Properties”).

REFERENCES

1. P. A. Bartolotta and D. L. Krause, in *Proceedings of the 2nd International Symposium on Gamma Titanium Aluminides* (TMS, San Diego, California, 1999), p. 3.
2. X. Wu, *Intermetallics* **14**, 1114 (2006).
3. C. Leyens, M. Peters, and W. A. Kaysser, *Surf. Coat. Technol.* **94–95**, 34 (1997).
4. A. Hirose, T. Ueda, and K. F. Kobayashi, *Mater. Sci. Eng. A* **160**, 143 (1993).
5. A. S. Ramos, R. Calinas, and M. T. Vieira, *Surf. Coat. Technol.* **200**, 6196 (2006).
6. S. PalDey, S. C. Deevi, and T. L. Alford, *Intermetallics* **12**, 985 (2004).
7. V. Budilov, R. Kireev, and Z. Kamalov, *Mater. Sci. Eng. A* **375–377**, 656 (2004).
8. I. A. Kurzina, E. V. Kozlov, Yu. P. Sharkeev, et al., *Surf. Coat. Technol.* **201**, 8463 (2007).
9. Y. Setsuhara, H. Ohsako, Y. Makino, and S. Miyake, *Surf. Coat. Technol.* **66**, 495 (1994).
10. I. A. Bozhko, I. A. Kurzina, I. B. Stepanov, and Yu. P. Sharkeev, *Fiz. Khim. Obrab. Mater.*, No. 4, 58 (2005).
11. T. V. Vakhnii, G. A. Verzhinin, I. A. Bozhko, et al., *J. Surf. Invest.* **2**, 301 (2008).
12. P. Staron, A. Bartels, H.-G. Brokmeier, et al., *Mater. Sci. Eng. A* **416**, 11 (2006).
13. S. Adachi and K. Nakata, *Surf. Coat. Technol.* **201**, 5617 (2007).
14. B. Guo, J. Zhou, S. Zhang, et al., *Appl. Surf. Sci.* **253**, 9301 (2007).
15. A. Hirose, T. Ueda, and K. F. Kobayashi, *Mater. Sci. Eng. A* **160**, 143 (1993).
16. V. P. Rotshtein, Yu. F. Ivanov, Yu. A. Kolubaeva, et al., *Tech. Phys. Lett.* **37**, 226 (2011).
17. A. D. Verkhoturov, *Formation of a Surface Layer of Metals in Spark Alloying* (Dal'nauka, Vladivostok, 1995) [in Russian].
18. E. I. Zamulaeva, E. A. Levashov, A. E. Kudryashov, et al., *Surf. Coat. Technol.* **202**, 3715 (2008).
19. A. V. Ribalko and O. A. Sahin, *Surf. Coat. Technol.* **201**, 1724 (2006).
20. S. V. Nikolenko and S. B. Ishchenko, RF Patent No. 2429953, *Byull. Izobret.* No. 27 (2011).

Translated by A. Kazantsev